Journal of Power Sources 251 (2014) 470–475

Contents lists available at ScienceDirect

Journal of Power Sources

journal homepage: www.elsevier.com/locate/jpowsour

Short communication

All-solid-state Al–air batteries with polymer alkaline gel electrolyte

Zhao Zhang, Chuncheng Zuo, Zihui Liu, Ying Yu, Yuxin Zuo*, Yu Song

College of Mechanical Science and Engineering, Jilin University, Changchun 130022, China

HIGHLIGHTS

- PAA-based alkaline gel electrolyte with a high ionic conductivity of 460 mS cm^{-1}.
- Peak capacity and energy densities of 1166 mAh g^{-1}-Al and 1230 mWh g^{-1}-Al.
- High area densities of 29.2 mAh cm^{-2} and 30.8 mWh cm^{-2} of the whole battery.
- High power density of 91.13 mW cm^{-2}.
- A novel separation design to inhibit anodic corrosion when not in use.

GRAPHICAL ABSTRACT

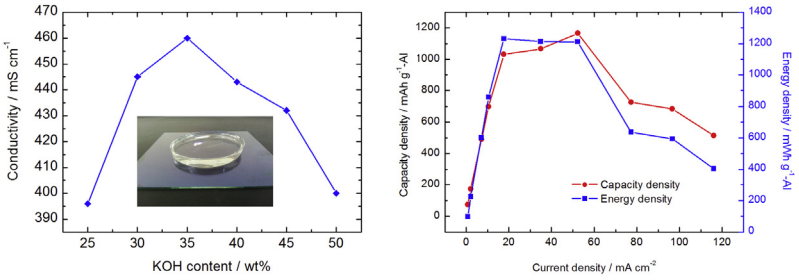

ARTICLE INFO

Article history:
Received 21 August 2013
Received in revised form
9 November 2013
Accepted 11 November 2013
Available online 20 November 2013

Keywords:
All-solid-state
Al–air battery
Polyacrylic acid
Alkaline gel electrolyte
Separation

ABSTRACT

Aluminum–air (Al–air) battery is one of the most promising candidates for next-generation energy storage systems because of its high capacity and energy density, and abundance. The polyacrylic acid (PAA)-based alkaline gel electrolyte is used in all-solid-state Al–air batteries instead of aqueous electrolytes to prevent leakage. The optimal gel electrolyte exhibits an ionic conductivity of 460 mS cm^{-1}, which is close to that of aqueous electrolytes. The Al–air battery peak capacity and energy density considering only Al can reach 1166 mAh g^{-1}-Al and 1230 mWh g^{-1}-Al, respectively, during constant current discharge. The battery prototype also exhibits a high power density of 91.13 mW cm^{-2}. For the battery is a laminated structure, area densities of 29.2 mAh cm^{-2} and 30.8 mWh cm^{-2} are presented to appraise the performance of the whole cell. A novel design to inhibit anodic corrosion is proposed by separating the Al anode from the gel electrolyte when not in use, thereby effectively maintaining the available capacity of the battery.

1. Introduction

Metal–air batteries have a much higher capacity and energy density than other energy storage devices, such as Li-ion, Ni–Cd, and lead-acid batteries [1]. Active metals, including Li, Ca, Mg, Al, Fe, and Zn, can be employed as anode materials. Al is an ideal candidate because of its trivalence and atomic weight of 26.98. The theoretical specific capacity of Al is up to 2.98 Ah g^{-1}-Al, which is second only to that of Li (3.86 Ah g^{-1}-Li). Al also exhibits a high energy density of 8.10 Wh g^{-1}-Al [2]. Furthermore, Al has attracted extended attention due to its abundance, low price, non-toxicity, and environmental friendliness.

A typical Al–air battery is composed of an Al anode, an air cathode and an alkaline or brine electrolyte. The half-cell reactions on both electrodes are expressed as:

$$\text{Anodic}: Al + 4OH^- \rightarrow Al(OH)_4^- + 3e^- \quad E^0 = -2.35\ V \qquad (1)$$

$$\text{Cathodic}: O_2 + 2H_2O + 4e^- \rightarrow 4OH^- \quad E^0 = +0.40\ V \qquad (2)$$

The overall Al–air battery reactions can be summarized as follows:

* Corresponding author. Tel./fax: +86 431 85095078.
E-mail address: yuxinzuo.jlu@gmail.com (Y. Zuo).

0378-7753/$ – see front matter © 2013 Elsevier B.V. All rights reserved.
http://dx.doi.org/10.1016/j.jpowsour.2013.11.020

$$4Al + 3O_2 + 6H_2O + 4OH^- \rightarrow 4Al(OH)_4^- \quad E^0 = 2.75\ V \qquad (3)$$

There exists a parasitic hydrogen evolution effect at the Al anode as follows:

$$2Al + 6H_2O + 2OH^- \rightarrow 2Al(OH)_4^- + 3H_2\uparrow \qquad (4)$$

The electrolyte plays an important role in Al–air batteries. It separates the anode and the cathode to avoid short circuit and simultaneously provides OH^- to maintain the electrochemical reactions. Aqueous electrolytes are widely used in metal–air batteries because of their high ionic conductivities. However, the fluidity may lead to the penetrations and leakages through the capillaries in the porous air cathode. Hydrophobic polytetrafluoroethylene (PTFE) emulsion or powder can be adulterated into the air-diffusion layer of the air cathode to inhibit the leakage [3,4]. But the PTFE may obstruct the diffusion of both gas and reactants, so An et al. proposed an agar chemical hydrogel electrode binder to enhance mass transport [5]. Recently, combining the aqueous electrolyte and the polymer gel has become a promising method to solve these problems. Othman and Mohamad used hydroponic gel to store alkaline electrolyte for Zn–air cells [6,7]. The hydroponics gel absorbed aqueous potassium hydroxide solution and expanded into loosely bound jelly granules. However, the interface between gel granules and the anode was not smooth enough. Polymer-gelling agents, such as polyvinylalcohol (PVA) [8,9] or polyethylene oxide (PEO) [10], can turn the aqueous electrolyte into a gel membrane. This kind of polymer electrolyte has a low thickness (50–250 μm), as well as chemical and thermal stability. However, the ionic conductivity of PVA- or PEO-based gel is quite limited. In literature the PVA alkaline solid polymer electrolyte exhibited an ionic conductivity under of 1×10^{-2} S cm^{-1} [11,12]. Wu et al. added acrylic acid (AA) to enhance the conductivity of PVA-based electrolyte to 0.142–0.301 S cm^{-1} [13]. Gaikwad obtained a highly viscous and conductive alkaline gel electrolyte by applying polyacrylic acid (PAA) as an additive in KOH solution [14]. Nevertheless, the electrolyte remained mobile, and a mesh structure support was necessary to hold the electrolyte. Cross-linked PAA exhibits an excellent balance between ionic conductivity and mechanism strength. Free-standing polymer gel electrolyte (PGE) films could be synthesized with PAA and KOH solution, and used in alkaline batteries [15]. However, to the best of our knowledge, there are few studies on gel electrolytes for Al–air batteries available in literature. The current study presents an application of an all-solid-state Al–air battery employing PAA-based alkaline gel electrolyte, which is simply prepared to obtain a relatively high conductivity.

In addition to leakages, the anodic corrosion is another obstacle to further commercialization of Al–air batteries [16,17]. Anode materials dissolve in alkaline electrolytes severely, thereby leading to the self-discharge. Meanwhile, parasitic hydrogen evolution may cause potential safety hazards. Thus, early Al–air batteries normally used low-concentration alkaline or neutral brine solutions as electrolytes to retard the corrosion rate, but the capacity and power densities of the battery were concurrently limited [18–20]. The Al anode can be discharged to 105.0 mAh g^{-1} and 5.5 mW cm^{-2} with 0.6 M KOH solution. Al alloy mixed with small amounts of Sn, In, or Zn can suppress corrosion [21,22]. The contact of In and Sn lead to micro-galvanic cells. The In ions dissolved into the solution and redeposit on the cathodic surface to decrease the hydrogen evolution. On the other hand, several corrosion inhibitors in the electrolyte, such as organic acids and ionic liquids, also exhibit good performance [23,24]. PAA, which is mentioned above as a polymer gel agent, is indicated to be a corrosion inhibitor for Al in electrolyte solutions [25,26]. Arthur and Umoren indicated that the polymer adsorbed on the surface of Al to suppress the corrosion in both alkaline and acid environment [27,28]. Amin et al. found that polymers with larger molecular weight had a better performance due to the stronger adsorption [29].

In this work a novel all-solid-state Al–air battery with PAA-based alkaline gel electrolyte is demonstrated as a substitute for aqueous energy storage devices. The following section presents a detailed process of electrolyte preparation and Al–air battery fabrication for reproducibility. In addition, the electrochemical characteristics of the electrolyte is measured and discussed. Furthermore, the discharge tests of the all-solid-state Al–air battery are carried out. Finally, a separation design is proposed to inhibit the Al corrosion when the battery is not in use.

2. Experimental

2.1. Materials

All materials used in this work were of analytical grade, and used without further treatment. Reagents for the electrolyte synthesis, including KOH, acrylic acid (AA), ZnO, $K_2S_2O_8$, and *N*,*N*′-methylene-bisacrylamide (MBA), were purchased from Sinopharm Chemical Reagent (Co., Ltd). The anode was made of a 0.2 mm thick, pure Al mesh with a real area ratio of 37.3%. For the air cathode, the activated carbon, ether black, Ni foam, and poly(vinylidene fluoride) (PVDF) were purchased from Shenyang Kejing. Catalyses including La_2O_3, SrO, and MnO_2 were from Tianjin Fuchen. And the organic solvent *N*-methyl-2-pyrrolidone (NMP) was provided by Sinopharm.

2.2. Synthesis of alkaline gel electrolyte

The alkaline gel electrolyte was obtained by casting a mixture of i) an alkaline solution, ii) a gel agent, and iii) a polymerization initiator onto a glass substrate and then polymerized. i) KOH (12 g) was dissolved in double distilled water (19 g), and then added with ZnO (0.4 g) to form an alkaline solution with pH 14.7. The ZnO additive in alkaline solutions was used as a corrosion inhibitor [30–33]. The solution was treated with ultrasonication bath until completely homogeneous. ii) The gel agent was composed of AA (2 g) with cross-linker MBA (0.3 g). iii) In addition, a 16 wt% $K_2S_2O_8$ solution (2 g) was used as the polymerization initiator. Firstly, the alkaline solution was added into the gel agent to obtain a slightly viscous liquid with white granular precipitates. The precipitates were then removed through percolation to obtain a clear and light yellow filtrate. Afterward, the polymerization initiator was dropped into the filtrate with continuously rapid stirring to colorless and clarity. The final solution was immediately poured into a petri dish (70 mm diameter) to form a liquid film of 3 mm thickness. After about 5 min polymerization at room temperature, the electrolyte was solidified to be transparent, elastic and freestanding. The thickness was almost the same as the liquid film before polymerization, which had been verified by Zhu et al. [34]. Gel electrolytes with different composites were synthesized in the same way for characterization comparison.

2.3. Fabrication methods

2.3.1. Al anode

The Al mesh was abraded with emery papers (400–800 grit) and then immersed in a 0.5 M KOH solution for 1 min to remove the oxide layer. The surface-treated specimen was rinsed with double distilled water and then dried using a filter paper. Finally the Al mesh was cut into a rectangle plate (40 × 30 mm) and soldered to a Ni current collector. Holes on the mesh were considered as escape channels for hydrogen generated during corrosion. Otherwise, the obstructed gas might form bubbles in the gel film to separate the

anode and electrolyte, thereby leading to the decay of battery performances.

2.3.2. Air cathode

Imitating the approaches of early researches [1,3,15,35], the porous air cathode was prepared by casting a cathodic paste onto a Ni foam. A mixture composed of conductive material (70 g of activated carbon and 10 g of ether black) and catalyst (8 g of La_2O_3, 2 g of SrO, and 10 g of MnO_2) was milled together with 8 g of PVDF as the polymer binder. The solid blend was dispersed in NMP to form a 400 mL viscous paste. The PVDF could bind electrode composites to the Ni foam tightly under room temperature [36]. The Ni foam was used as both mechanical support and current collector, stuffed with the cathodic paste. After drying for 24 h at ambient temperature, it was pressed at 8 MPa to form a 0.3 mm thick cathode plate. A smooth surface was obtained by the cold press process to contact with the gel electrolyte film sufficiently. Micro pores were formed due to the evaporation of the NMP solvent, through which air could penetrate into the porous cathode.

2.3.3. Battery assembling

The alkaline gel electrolyte film was sandwiched between an Al anode mesh and an air cathode plate, as shown in Fig. 1A. The laminar structure was easy to fabricate and refuel by replacing the Al mesh.

2.4. Measurements

The conductivity is one of the most important characteristic of electrolytes, which is affected by the content of KOH and AA. AA monomer weights of 0, 5, 10, and 15 g were dissolved in 50 g of distilled water, separately. KOH pellets were gradually added into the solution and the conductivities were measured at each time. A pair of Pt electrodes was immersed in the electrolyte solution to measure the conductivity using a DDSJ-318 conductivity testing system from Shanghai Leici Co., Ltd.

To investigate the conductivity of the polymer alkaline gel electrolyte film, the Pt electrodes was immersed in the AA–KOH solution with MBA before the $K_2S_2O_8$ was added. This was to ensure the close contact between electrodes and the electrolyte. Measurements were carried out on the electrolytes after solidification in the presence of the initiator.

The completely assembled Al–air battery prototype was tested to demonstrate its discharge characteristics using a NEWARE BTS-5V3A battery testing system. Discharging curves were recorded with constant current densities from 0.7 mA cm^{-2} to 116 mA cm^{-2}. In addition, an intermittent discharging experiment was carried out at 50 mA cm^{-2} with a 20-min rest to investigate the self-discharging performance.

3. Results and discussion

3.1. Polymerization proceeding

Polymer agents were composed in the electrolyte to enhance its mechanical properties. The PAA-based alkaline gel electrolyte was prepared by polymerizing AA monomers into polymer chains, and then cross-linked to form a 3 dimensional matrix structure that can store the aqueous electrolyte. The free-radical polymerization process is illustrated in Fig. 1B. The whole process was highly exothermic. The increase in the AA monomer concentration can lead to enhancements in both PAA molecular weight and mechanical strength of the gel. The cross-linker MBA content affects the mechanical strength and the flexibility of the gel electrolyte [34]. The solidification is insufficient with MBA less than 0.5 wt%, whereas the gel loses elasticity above 1.4 wt%. The gelation speed depends on the content of the initiator. The more $K_2S_2O_8$ added, the higher gelation speed was obtained. In this study, a highly concentrated initiator solution is used to achieve a solidification time of less than 5 min. Thus, the gel agent should be sufficiently stirred to avoid inhomogeneity.

3.2. Ionic conductivity

In the PAA-based alkaline gel electrolyte system, the conductivity exhibits as a function of AA monomer and KOH contents. First, we present the effect of KOH concentration with fixed AA contents. Fig. 2 shows the conductivity curves versus the KOH mass fraction with different AA contents. An inflection point is observed on each curve with a KOH:AA mole ratio of 1:1 (except for 0 g of AA) to form potassium acrylate (AA–K) exactly. Afterward, the slopes increase significantly because of the complete ionization of KOH. The highest conductivities appear at KOH contents 35.06, 36.52, 35.80, and 35.94 wt% for 0, 5, 10, and 15 g of AA, respectively. Excess KOH beyond the peak concentration can inhibit the conductivity of the solution because of increased viscosity and restricted ion mobility [37–39]. Thus, the KOH content is fixed at 36 wt% in the following research. The conductivity linearly decreases with increasing AA monomer fraction (Fig. 3). AA monomers can be polymerized as PAA chains in the presence of the initiator. The comparison between AA–KOH and PAA–KOH solutions is carried out to present negligible differences in conductivities. Thus, a compromising AA monomer content of 6 wt% is chosen, taking account of both mechanical and electrochemical performances. The conductivity of

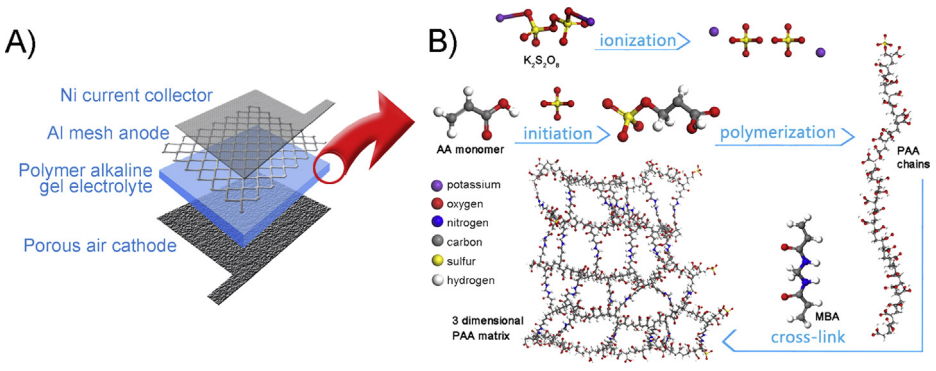

Fig. 1. Schematic all-solid-state Al–air battery with a laminar structure. B) Illustration of the polymerization process from AA monomers to a PAA matrix. Particles represent different atoms distinguished by color, *white* for hydrogen, *gray* for carbon, *red* for oxygen, *yellow* for sulfur, *blue* for nitrogen, and *purple* for potassium, respectively.

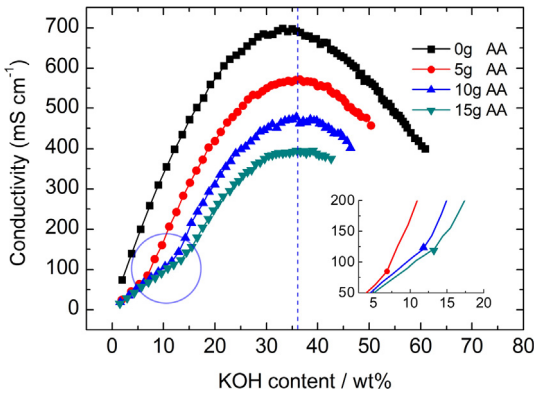

Fig. 2. Conductivity as a function of KOH content at 25 °C with 0, 5, 10, and 15 g of AA, respectively. The *dashed line* indicates the KOH content at 36 wt%. The insert is the partial graph to present the inflection points.

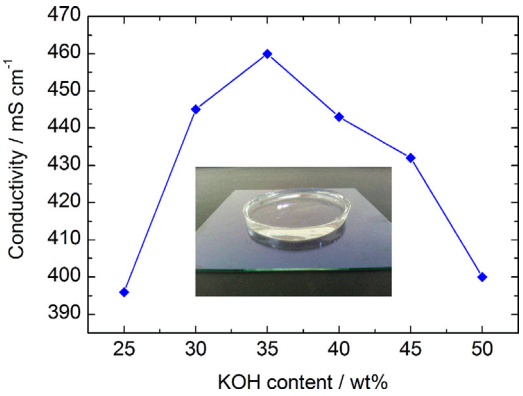

Fig. 4. Conductivity curve of a polymer alkaline gel electrolyte with 6 wt% PAA at 25 °C. The insert is a photograph of the colorless, transparent, and elastic electrolyte gelatin.

such a solution is up to 563 mS cm^{-1}, which is 77.2% of the KOH aqueous solution without a polymer agent.

The conductivity of polymer gel electrolyte is always lower than that of aqueous KOH solutions. This phenomenon is due to that a portion of water is bound in the polymer matrix, and thus the fraction of free water that can transport ions is limited. Palaniappan listed the conductivities of various alkaline polymer gel electrolytes to find the highest value of 288 mS cm^{-1} [40]. Wu et al. presented a PVA/PAA polymer electrolyte with the conductivity of 301 mS cm^{-1}, which is the best achievement to the best of our knowledge [41]. In this work, a 36% decline is observed for the gel electrolyte compared with the liquid solution. Finally, as shown in Fig. 4, an optimal conductivity of 460 mS cm^{-1} at 25 °C is achieved with the composition mentioned in Sec. 2.2.

3.3. Discharge performance

The discharging performances were tested with constant currents from 0.7 mA cm^{-2} to 116 mA cm^{-2}. The discharging voltages remain stable when the current density is less than 20 mA cm^{-2} (Fig. 5A). The sharp decline at the end of the discharge process indicates that the amount of Al is exhausted and the electrolyte is in excess. Above the 30 mA cm^{-2} region, the voltage decreases over time because of the insufficient ion diffusion in the electrolyte (Fig. 5B). Fig. 6 exhibits the discharging voltage profiles at different current densities. The black curve represents the peak voltage, whereas the red (in the web version) curve denotes the average voltages during the entire discharge process. The voltage decline is due to the ohmic polarization. The power density (blue curve) is significantly promoted with increasing current density.

The discharging current also affects the available capacity and energy densities of the battery, as shown in Fig. 7. The energy density profile has a similar tendency with that of the capacity density profile because of the relatively stable operating voltage. Considering only the weight of Al consumed during discharging, the highest capacity is up to 1166 mAh g^{-1}-Al when it is discharged at 52 mA cm^{-2}. In addition, the peak energy density 1230 mWh g^{-1}-Al is obtained at 18 mA cm^{-2}. Compared with the previous results using weak alkaline electrolyte (0.6 M KOH, 105 mAh g^{-1} at 0.8 mA cm^{-2}) [42] and neutral brine electrolyte (3.5% NaCl, 1340 mAh g^{-1} at 1.8 mA cm^{-2}) [43], both of these

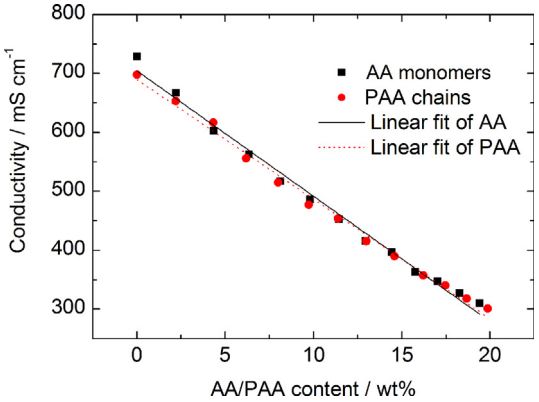

Fig. 3. Conductivity as a function of AA/PAA content with 36 wt% KOH at 25 °C. The two linear fitting results almost coincide with each other.

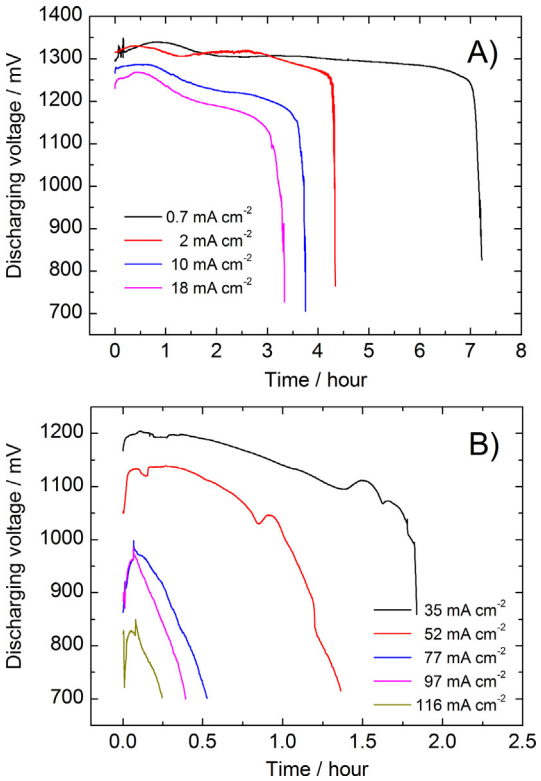

Fig. 5. Discharging voltage profiles with a constant current density below 20 mA cm^{-2} (A) and above 30 mA cm^{-2} (B).

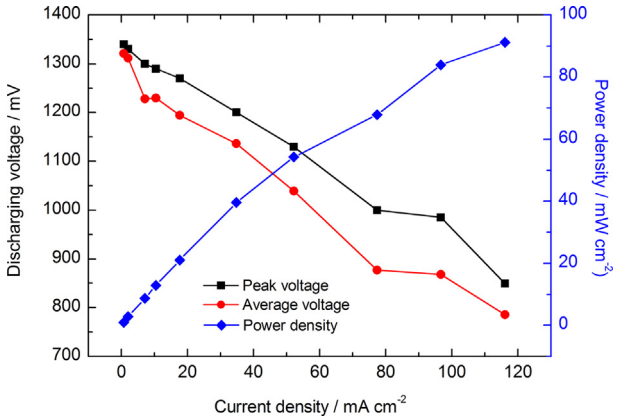

Fig. 6. Discharging voltage and power density profiles versus current density.

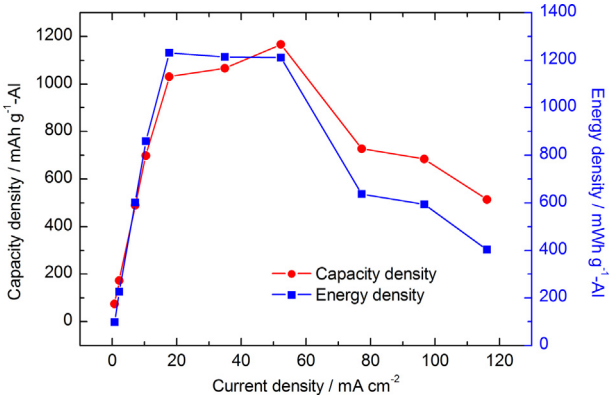

Fig. 7. Capacity and energy density profiles during constant current discharge.

achievements show a relatively high utilization of Al material and are impressive for substantial applications. It should be noticed that the Al–air battery is a laminated structure with small thickness, so the area capacity and energy densities are necessary to appraise the performance of the whole cell. The peak area densities of 29.2 mAh cm^{-2} and 30.8 mWh cm^{-2} are corresponding to the discharging currents mentioned above, respectively. An abnormal phenomenon is observed with current densities below 20 mA cm^{-2}, wherein the capacity is quite limited. A possible explanation for this behavior is that in the long discharging time (more than 3 h), a high fraction of Al is consumed dissolving into the electrolyte, as known as self-discharging. Although the polymer alkaline gel electrolyte has been indicated to show excellent performance in anodic protection, Al corrosion cannot be ignored especially during low current discharging or rest.

In this study, we propose a simple method by completely separating the Al anode from the gel electrolyte when not in use to avoid Al depletion. An illustration of the separable battery design is presented in Fig. 8A. The Al mesh and Ni current collector are set into a sliding block. The sliding block can be moved along the sliding guide on the cell shell with control bars. The electrolyte film and the air cathode are fixed on the cell cover. After assembled, the Al mesh is in contact with the electrolyte film to discharge (Fig. 8B). During rest, the sliding block is moved away from the electrolyte, and then the Al mesh and the electrolyte film are separated (Fig. 8C). The re-jointing process is in a reversed way. The surface of the Al electrode is free of wetness so that it needs no more treatment at all after separation. However, this process is impossible for traditional liquid electrolyte systems. An intermittent discharging experiment was carried out at 50 mA cm^{-2} with a 20-min rest between two discharging processes (Fig. 9). In case of the non-separated battery, the voltage decreases rapidly when it is discharged to 760.8 mAh g^{-1}-Al. By contrast, the prototype with the separation design shows a capacity density of 1093.8 mAh g^{-1}-Al, which is close to that during continuous discharging.

4. Conclusions

In this study, an all-solid-state Al–air battery with PAA-based alkaline gel electrolyte was presented to achieve high capacity and energy densities and avoid leakage simultaneously. The gel electrolyte was prepared using a simple polymerization method. The ionic conductivity of the gel electrolyte is primarily determined by the contents of KOH and the polymer agent. An optimal composition of 36 wt% KOH and 6 wt% AA is confirmed to obtain the balance between mechanism strength and conductivity. The final conductivity of the gel electrolyte reached 460 mS cm^{-1}. The all-solid-state Al–air battery is a laminar structure composed of an Al anode, a polymer alkaline gel electrolyte film, and a porous air cathode. Constant current discharge tests have been performed, and the peak capacity and energy density are up to 1166 mAh g^{-1}-Al and 1230 mWh g^{-1}-Al, respectively. The battery prototype also exhibits a high power density of 91.13 mW cm^{-2}. The peak area capacity and energy densities, 29.2 mAh cm^{-2} and 30.8 mWh cm^{-2} are calculated to appraise the laminated battery with small thickness. To inhibit the self-discharging caused by anodic corrosion, a novel separation design is proposed in this paper. The Al anode is separated from the electrolyte film when not in use to maintain the available capacity.

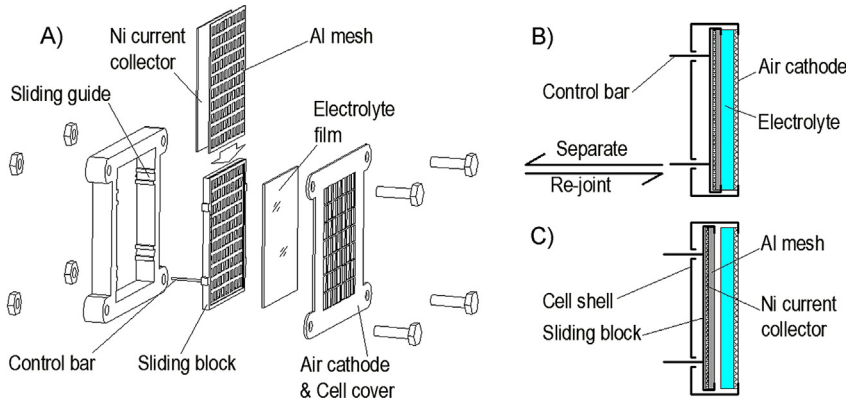

Fig. 8. Illustration of the separable battery (A). The Al anode in contact with the electrolyte film (B) and separated from the electrolyte film (C), respectively.

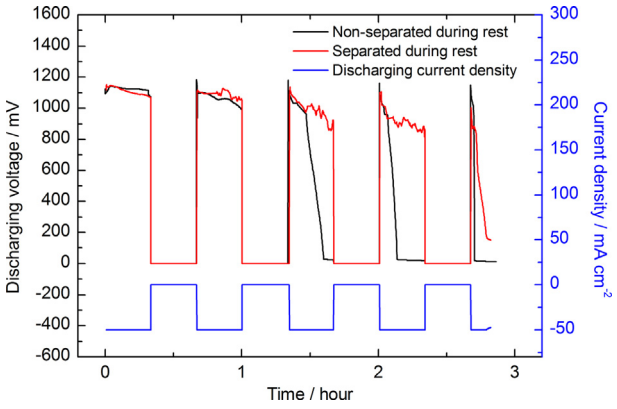

Fig. 9. Intermittent discharge performance. The separation of the anode and the electrolyte during rest can effectively avoid Al depletion. The negative sign of the current density indicates the discharge process.

The intermittent discharge experiment results indicate that the separation could promote the Al utilization effectively.

Acknowledgments

This work was supported by the National Natural Science Foundation of China (No. 51175223) and the Science and Technology Planning Project of Jilin Province (No. 20100564).

References

[1] J.S. Lee, S.T. Kim, R. Cao, N.S. Choi, M. Liu, K.T. Lee, J. Cho, Adv. Energy Mater. 1 (2011) 34.
[2] S. Yang, H. Knickle, J. Power Sources 112 (2002) 162.
[3] S.I. Smedley, X.G. Zhang, J. Power Sources 165 (2007) 897.
[4] N. Gupta, T. Toh, M.W. Fatt, S. Mhaisalkar, M. Srinivasan, J. Solid State Electrochem. 16 (2012) 1585.
[5] L. An, T.S. Zhao, L. Zeng, Appl. Energy 109 (2013) 67.
[6] R. Othman, A.H. Yahaya, A.K. Arof, J. Appl. Electrochem. 32 (2002) 1347.
[7] A.A. Mohamad, J. Power Sources 159 (2006) 752.
[8] J.F. Drillet, M. Adam, S. Barg, A. Herter, D. Kock, V.M. Schmidt, M. Wilhelm, ECS Trans. 28 (2010) 13.
[9] G. Merle, S.S. Hosseiny, M. Wessling, K. Nijmeijer, J. Membr. Sci. 409 (2012) 191.
[10] S.S. Sekhona, D.P. Kaura, J.S. Parkb, K. Yamada, Electrochim. Acta 60 (2012) 366.
[11] A.A. Mohamad, N.S. Mohamed, M.Z.A. Yahya, R. Othman, S. Ramesh, Y. Alias, A.K. Arof, Solid State Ionics 156 (2003) 171.
[12] C.C. Yang, S.J. Lin, S.T. Hsu, J. Power Sources 122 (2003) 210.
[13] G.M. Wu, S.J. Lin, C.C. Yang, J. Membr. Sci. 275 (2006) 127.
[14] A.M. Gaikwad, A.M. Zamarayeva, J. Rousseau, H. Chu, I. Derin, D.A. Steingart, Adv. Mater. 24 (2012) 5071.
[15] G.Q. Zhang, X.G. Zhang, Electrochim. Acta 49 (2004) 873.
[16] S.I. Pyun, S.M. Moon, J. Solid State Electrochem. 4 (2000) 267.
[17] H. Wang, D.Y.C. Leung, M.K.H. Leung, M. Ni, Energy Fuels 24 (2010) 3748.
[18] R. Othman, W.J. Basirun, A.H. Yahaya, A.K. Arof, J. Power Sources 103 (2001) 34.
[19] M. Nestoridi, D. Pletcher, R.J.K. Wood, S. Wang, R.L. Jones, K.R. Stokes, I. Wilcock, J. Power Sources 178 (2008) 445.
[20] I. Smoljko, S. Gudic, N. Kuzmanic, M. Kliskic, J. Appl. Electrochem. 42 (2012) 969.
[21] Y. Tang, L. Lu, H.W. Roesky, L. Wang, B. Huang, J. Power Sources 138 (2004) 313.
[22] S. Gudic, I. Smoljko, M. Kliskic, J. Alloys Compd. 505 (2010) 54.
[23] K. Kim, Y.H. Cho, S.W. Eom, H.S. Kim, J.H. Yeum, Mater. Res. Bull. 45 (2010) 262.
[24] J.M. Wang, J.B. Wang, H.B. Shao, X.X. Zeng, J.Q. Zhang, C.N. Cao, Mater. Corros. 60 (2009) 977.
[25] H. Zhu, Z. Chen, Y. Sheng, T.T.L. Thi, Dyes Pigm. 86 (2010) 155.
[26] S.A. Umoren, Y. Li, F.H. Wang, J. Appl. Electrochem. 41 (2011) 307.
[27] D.E. Arthur, A. Jonathan, P.O. Ameh, C. Anya, Int. J. Ind. Chem. 4 (2013) 2.
[28] S.A. Umoren, Y. Li, F.H. Wang, J. Solid State Electrochem. 14 (2010) 2293.
[29] M.A. Amin, S.S.A. EI-Rehim, E.E.F. El-Sherbini, O.A. Hazzazi, M.N. Abbas, Corros. Sci. 51 (2009) 658.
[30] A.M. Gaikwad, G.L. Whiting, D.A. Steingart, A.C. Arias, Adv. Mater. 23 (2011) 3251.
[31] Q. Li, N.J. Bjerrum, J. Power Sources 110 (2002) 1.
[32] L. Bockstie, D. Trevethan, S. Zaromb, J. Electrochem. Soc. 110 (1963) 267.
[33] R.S.M. Patnaik, S. Ganesh, G. Ashok, M. Ganesan, V. Kapali, J. Power Sources 50 (1994) 331.
[34] X. Zhu, H. Yang, Y. Cao, X. Ai, Electrochim. Acta 49 (2004) 2533.
[35] G.M. Wu, S.J. Lin, C.C. Yang, J. Power Sources 244 (2013) 287.
[36] N. Singh, C. Galande, A. Miranda, Sci. Rep. 2 (2012) 481.
[37] C. Iwakura, S. Nohara, N. Furukawa, H. Inoue, Solid State Ionics 148 (2002) 487.
[38] P.L. Ng, A. Jamaludin, Y. Alias, W.J. Basirun, Z.Z. Ahmad, A.A. Mohamad, J. Appl. Polym. Sci. 123 (2012) 2662.
[39] S. Yashonath, P.K. Ghorai, J. Phys. Chem. B 112 (2008) 665.
[40] R. Palaniappan, G.G. Botte, Electrochim. Acta 88 (2003) 772.
[41] G.M. Wu, S.J. Lin, C.C. Yang, J. Membr. Sci. 280 (2006) 802.
[42] A.A. Mohamad, Corros. Sci. 50 (2008) 3475.
[43] B. Han, G. Liang, Rare Met. 25 (2006) 360.